

## Chalcones induce apoptosis, autophagy and reduce spreading in osteosarcoma 3D models

M. Rossi<sup>a,b</sup>, C. Pellegrino<sup>a</sup>, M.M. Rydzyk<sup>a,b</sup>, G. Farruggia<sup>a,b</sup>, D. de Biase<sup>a,c</sup>, S. Cetrullo<sup>d,e</sup>, S. D'Adamo<sup>d</sup>, A. Bisi<sup>a</sup>, P. Blasi<sup>a,b</sup>, E. Malucelli<sup>a</sup>, C. Cappadone<sup>a,\*</sup>, S. Gobbi<sup>a</sup>

<sup>a</sup> Department of Pharmacy and Biotechnology, Alma Mater Studiorum University of Bologna, Bologna 40127, Italy

<sup>b</sup> Center for Applied Biomedical Research (CRBA), Alma Mater Studiorum University of Bologna, Bologna 40126, Italy

<sup>c</sup> Solid Tumor Molecular Pathology Laboratory, IRCCS Azienda Ospedaliero-Universitaria di Bologna, Bologna 40138, Italy

<sup>d</sup> Department of Biomedical and Neuromotor Sciences, Alma Mater Studiorum University of Bologna, Bologna 40138, Italy

<sup>e</sup> Istituto Nazionale per le Ricerche Cardiovascolari, Bologna 40126, Italy

### ARTICLE INFO

#### Keywords:

Spheroids  
MG-63  
143B  
Invasiveness  
Licochalcone A  
Antiproliferative activity

### ABSTRACT

Osteosarcoma is the most common primary bone malignancy with a challenging prognosis marked by a high rate of metastasis. The limited success of current treatments may be partially attributed to an incomplete understanding of osteosarcoma pathophysiology and to the absence of reliable *in vitro* models to select the best molecules for *in vivo* studies. Among the natural compounds relevant for osteosarcoma treatment, Licochalcone A (Lic-A) and chalcone derivatives are particularly interesting. Here, Lic-A and selected derivatives have been evaluated for their anticancer effect on multicellular tumor spheroids from MG63 and 143B osteosarcoma cell lines. A metabolic activity assay revealed Lic-A, **1i**, and **1k** derivatives as the most promising candidates. To delve into their mechanism of action, caspase activity assay was conducted in 2D and 3D *in vitro* models. Notably, apoptosis and autophagic induction was generally observed for Lic-A and **1k**. The invasion assay demonstrated that Lic-A and **1k** possess the ability to mitigate the spread of osteosarcoma cells within a matrix. The effectiveness of chalcone as a natural scaffold for generating potential antiproliferative agents against osteosarcoma has been demonstrated. In particular, chalcones exert their antiproliferative activity by inducing apoptosis and autophagy, and in addition they are capable of reducing cell invasion. These findings suggest Lic-A and **1k** as promising antitumor agents against osteosarcoma cells.

### 1. Introduction

Osteosarcoma (OS) is a primary malignant bone tumor affecting mainly children and adolescents, known for its high aggressiveness. Current therapeutic approaches involve chemotherapy and local surgery for primary lesions. Despite this, the overall patient survival rate has remained stable over the past 30 years [1,2]. Patients with localized primary tumors at diagnosis exhibit a 5-year survival rate of over 60 %, while those facing metastatic tumors have a survival rate of 20 %. Hence, there is a pressing need to develop novel anticancer drugs targeting OS to enhance patient survival [1,3].

The limited success of existing treatments may be partially attributed to an incomplete understanding of OS pathophysiology and the lack of reliable *in vitro* models to test the efficacy of new compounds before proceeding with *in vivo*/clinical studies [4]. Thus, a switch from 2D to

3D *in vitro* tumor models, such as multicellular tumor spheroid (MCTS), is necessary to better elucidate OS disease and to have more trustworthy assays. Indeed, a suitable *in vitro* model should accurately replicate the tumor microenvironment (TME). The traditional 2D cell cultures fall short in recapitulating several tumor features, such as tumor heterogeneity and tissue architecture [5,6]. On the other hand, 3D cultures enable a more faithful reproduction of the dynamic cell-cell and cell-extracellular matrix (ECM) interactions present in the TME, leading to a more accurate and reproducible early-stage testing for *in vivo*/clinical studies [7,8].

In the context of new potential anticancer treatments, natural products have historically been a valuable source of effective therapeutics and, among them, chalcones play a crucial role [9–11]. These compounds feature a chemical scaffold that can be found in many plant products, including spices, vegetables, fruits, and teas [12,13].

\* Corresponding author.

E-mail address: [concettina.cappadone@unibo.it](mailto:concettina.cappadone@unibo.it) (C. Cappadone).

<https://doi.org/10.1016/j.bioph.2024.117284>

Received 9 May 2024; Received in revised form 2 August 2024; Accepted 8 August 2024

Available online 15 August 2024

0753-3322/© 2024 The Authors. Published by Elsevier Masson SAS. This is an open access article under the CC BY-NC license (<http://creativecommons.org/licenses/by-nc/4.0/>).

Chalcones are members of the flavonoid family, which display a large structural diversity and can be readily synthesized [14]. Upon appropriate functionalization, they can interfere with multiple molecular targets exhibiting a wide range of activities, including anticancer, anti-inflammatory, antioxidant, and antimicrobial [15]. Interestingly, different chalcones have been approved for clinical use in various health conditions: *metochalcone* is employed as choleric and diuretic, *hesperidin methylchalcone* as vascular protective agent, and *sofalcone-based derivatives* as anti-ulcer and mucoprotective drugs [13–17].

Among natural chalcones, Licochalcone A (**Lic-A**), generally extracted from the roots of *Glycyrrhiza* species, is gaining attention for its antitumor activity. **Lic-A** effectiveness has been substantiated through *in vitro* studies on 2D cell culture, showing anticancer properties not only in OS [18–20] but also in other solid tumors [21–24]. Indeed, **Lic-A** suppresses OS cell proliferation through apoptosis and autophagy [18–20]. Apoptosis acts by disassembling damaged or unnecessary cells, while autophagy contributes to cellular homeostasis by selectively recycling organelles and intracellular molecules. However, under certain conditions, both processes can support the action of anti-cancer drugs in different and complementary ways [25].

In a previous work we demonstrated the antitumor capability of **Lic-A** and a series of synthesized chalcone derivatives on the MG63 OS cell line [18]. Here, we present the results of the antitumor efficacy of selected compounds, including **Lic-A**, on two different OS 3D models, giving insight into their antiproliferative mechanism of action.

## 2. Materials and methods

### 2.1. Cell culture and treatments

The MG63 and 143B OS cell lines were purchased from ATCC (American Type Culture Collection, Manassas, VA, USA). Cells were routinely grown in 5 % CO<sub>2</sub>/humidified air at 37 °C with Dulbecco's modified Eagle medium supplemented with D-glucose (4.5 g/L), 10 % fetal bovine serum (v/v), L- glutamine (2 mM), penicillin (1000 U/mL) and 1 mg/mL of streptomycin (Microtech, Pozzuoli, Italy).

Syntheses and structures of the tested chalcone derivatives were previously described by Rossi et al. [18]. Cells were treated with **Lic-A** and seven of the most promising compounds (**1e**, **1h**, **1i**, **1k**, **1o**, **1q** and **1r**). In all the experiments in the control condition the same amount of vehicle DMSO (Dimethyl sulfoxide, Merck KGaA, Darmstadt, Germany) was added.

### 2.2. MTT assay

Cellular metabolic activity, as an indicator of cell viability and cytotoxicity, was measured by an MTT assay on 143B cells. Briefly, cells were seeded at a density of 5000 cells/well in a 96-well plate and left to adhere overnight. The following day 143B cells were treated with **Lic-A** and the seven selected compounds at 80, 40, 20, 10, 5, 2.5, 1.25, 0.6125 μM. 48 h after the treatment, 10 μL of a 5 mg/mL MTT solution (Merck KGaA, Darmstadt, Germany) were added to each well and the plate was incubated for 2 h at 37 °C. Then, the cell culture medium was removed, and the formazan crystals formed were solubilized by adding 150 μL/well of propan-2-ol (Merck KGaA, Darmstadt, Germany). The absorbance at 570 nm was measured with an EnSpire® multimode plate reader (PerkinElmer, Waltham, USA). The sample absorbance at 690 nm was used as reference wavelength for correction. The half-maximal inhibitory concentration (IC<sub>50</sub>) was determined using the log (inhibitor) vs. response-variable slope (four parameter) function of GraphPad Prism software (version 6, GraphPad Software, San Diego, CA, USA).

### 2.3. Multicellular tumor spheroids

Multicellular tumor spheroids (MCTS) were generated from both cell lines by growing cell suspensions in an Ultra-Low Attachment

BIOFLOAT 96-well plate (faCellitate, Mannheim, Germany). To obtain single spheroids of uniform size, three cell seeding densities (4000, 2000, and 500 cells per well) were tested. To accelerate cell sedimentation and aggregation, a centrifugation step was carried out immediately after cell seeding (100 g x 3 minutes) and then incubated at 37 °C 5 % CO<sub>2</sub>. To analyze spheroid sizes, MCTS were also monitored by the IncuCyte® live-cell analysis system (Essen BioScience Ltd, Hertfordshire, UK). Phase images were then acquired every 6 h for 4 days and the dimension and roundness of the MCTS were calculated through the IncuCyte® ZOOM software.

### 2.4. Spheroids treatment

MCTS were treated with different concentrations of **Lic-A** and the selected chalcones (160, 80, 40, 20, 10, 5 μM) 3 days after seeding. After 72 h from treatment, cell viability was estimated using the resazurin assay. Briefly, the cell culture medium was replaced with a fresh one containing 100 μM resazurin (TCI, Milan, Italy). After 6 h of incubation the medium was collected and the fluorescence was measured by a plate reader (EnSpire® Multimode Plate Reader, Perkin-Elmer) applying a λ<sub>exc</sub> 560 nm and λ<sub>em</sub> 590 nm. Finally, the percentage of resazurin reduction was determined using the equation:

$$\frac{\text{fluorescence intensity sample} \times 100}{\text{fluorescence intensity basal medium}}$$

### 2.5. Viability determination

To verify not only the metabolic activity but also the viability, MCTS treated with 120 μM of **Lic-A**, **1i** and **1k** for 72 h were stained with propidium iodide for 30 minutes at the final concentration of 5 μg/mL. Images were acquired through fluorescence confocal microscopy (Nikon, Eclipse C1, Nikon instrument S.p.A, FI, Italy),

### 2.6. Caspase activity assay on 3D cell culture

In 3D models the activation of caspases was assessed by monitoring the cleavage of the fluorogenic peptide substrate Ac-Asp-Glu-Val-Asp-7-amido-4-methylcoumarin (Ac-DEVD-AMC), measuring the accumulation of a fluorescent product according to the procedure outlined in a previous work [26]. This substrate is recognized by caspase 3 and other effector caspases. In summary, cells were collected in Ripa Lysis and Extraction Buffer (Thermo Fisher Scientific, Waltham, MA, USA), subjected to sonication, followed by centrifugation for 10 minutes at 12000g at 4 °C. The resulting supernatant was employed to assess enzyme activity. Protein extracts were mixed with the assay buffer containing 100 mM Hepes pH 7; 5 mM dithiothreitol; 0.1 % (v/v) CHAPS; 10 % (w/v) sucrose; and 150 μM Ac-DEVD-AMC, then incubated for 15 minutes at 37 °C. The reaction was halted on ice by adding 2 % (w/v) sodium acetate in 0.2 M acetic acid. Subsequently, the release of 7-amino-4-methylcoumarin (AMC) was quantified in a post-sample dilution applying a λ<sub>exc</sub> 370 nm and λ<sub>em</sub> 455 nm. Fluorescence intensity was normalized per mg of protein and expressed as a fold increase over the untreated control.

### 2.7. Western blot analysis

Assessment of autophagy was carried out by evaluating the modulation of key autophagic proteins by western blot as previously described [27]. After 72 h of incubation from seeding, the spheroids were treated with **Lic-A**, **1i**, and **1k** at a concentration of 120 μM, or with the same amount of DMSO as in the control condition. Each treatment was performed with or without chloroquine (CQ) diphosphate salt (C6628, Merck KGaA, Darmstadt, Germany). The latter was reconstituted in PBS obtaining a 96.9 mM stock solution and used at a concentration of 25 μM. After 24 h of treatment, 24 MCTS per condition were collected

and centrifuged at 800 g for 5 minutes at 4 °C. Finally, they were suspended in 75 µL of Lysis Ripa Buffer supplemented with the Halt™ Protease and Phosphatase Inhibitor Cocktail (Thermo Fisher Scientific, Waltham, MA, USA), sonicated, and centrifuged for 10 minutes at 12000 g at 4 °C. After protein quantification by the Bradford method, equal amounts (20 µg) of cell extracts were subjected to electrophoresis in 15 % gels and blotted onto nitrocellulose membranes. The latter were saturated in Tris-Buffered Saline containing 0.05 % Tween 20 (TBS-T) and 5 % milk for 1 h at room temperature and probed with primary antibodies at 4 °C overnight, specifically targeting LC3 (Cell Signaling Technology, Danvers, Massachusetts, USA, Rabbit anti- LC3A/B Pab#4108) and p62 (Santa Cruz Biotechnology, Dallas, TX, USA, mouse monoclonal #SC28359). Actin (Thermo Fisher Scientific, Waltham, MA, USA, #MA5-11869) served as a loading control and for the normalization of band intensity. After washes, membranes were incubated with horseradish peroxidase-conjugated anti-rabbit (Cell Signaling Technology, Danvers, Massachusetts, USA) or anti-mouse (Santa Cruz Biotechnology, Dallas, TX, USA) IgG for 1 h at room temperature. The chemiluminescent signals were detected using Immobilon Forte Western HRP substrate (Millipore, # WBLUF0500) and acquired by the ChemiDoc™ Imaging System. The combined evaluation of LC3 and p62 immunoblotting was undertaken following the guidelines detailed by Klionsky et al. [28] for a correct evaluation of autophagy and the assessment of the autophagic flux.

## 2.8. Invasion assay

To determine the ability of Lic-A and the studied chalcones to inhibit OS cells spreading through a matrix, an invasion assay was performed. After spheroid generation, culture media was replaced with 75 µL of Matrigel® (Corning, NY, USA) diluted 1:1 with cell culture media containing the different treatments in order to reach the final concentration of 120 µM. After 45 minutes of incubation at 37 °C to allow Matrigel gelation, 50 µL of fresh medium were added on top. The Plate was then incubated in an IncuCyte® live-cell analysis system (Essen BioScience Ltd, Hertfordshire, UK). Phase images were then acquired every 6 h for three days. Finally, the whole MCTS dimension and the invading cell area were calculated through the IncuCyte® ZOOM software.

## 2.9. Statistical analysis

Data are reported as means ± SD of at least three independent experiments and all treatments were analyzed against control. A paired t-test, a Friedman test or a one and two-way ANOVA corrected for multiple comparisons (Dunn test) was performed with GraphPad Prism software (GraphPad Software, version 6.0c, San Diego, CA, USA) ([www.graphpad.com](http://www.graphpad.com)). Significance was graphically reported as follows: \* p < 0.05, \*\* p < 0.01, and \*\*\* p < 0.001.

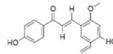
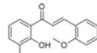
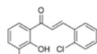
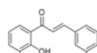
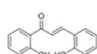
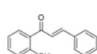
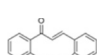
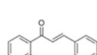
## 3. Result and discussion

### 3.1. The antiproliferative effect of chalcones on 2D cell culture models

Here we report the IC<sub>50</sub> of Lic-A and seven chalcones on 143B cell culture, a well-known aggressive and metastatic OS cell line [29]. In a previous work, we selected the seven chalcones on the basis of their antitumor activity on MG63 OS cell line (Table 1) [18] and these data are reported for comparison.

MG63 and 143B remained 'stable' without external contamination during *in vitro* expansion as shown by next generation sequencing (NGS) analysis [30]. No discrepancies were observed regarding the presence of single nucleotide variants and variant allele frequency (Table 1 SI), ensuring that the cell lines were suitable for testing anticancer activity without misinterpretation due to innate mutations. The NGS-based method has a significant sensitivity (≤ 5 %) and it can be used to authenticate human cell lines, xenografts and organoids.

**Table 1**  
Structures and IC<sub>50</sub> values of studied compounds on 2D culture.

Cpd	Structure	IC <sub>50</sub> µM (95 % CI) MG63 <sup>a</sup>	IC <sub>50</sub> µM (95 % CI) 143B
Lic-A		10.4 (9.4 – 11.4)	18.1 (15.6–21)
1e		42.5 (22.9 – 78.8)	18.9 (16–22.3)
1h		17.0 (15.4 – 18.9)	14.1 (13–15.3)
1i		12.7 (11.5 – 14.0)	13.5 (12.2–15)
1k		14.5 (12.0 – 17.5)	15.5 (13.5–17.6)
1o		13.8 (12.4 – 15.3)	11.0 (10.2–11.8)
1q		10.6 (10.2 – 11.1)	7.0 (6.2–7.8)
1r		12.2 (11.6 – 12.8)	10.5 (9.8–10.9)

<sup>a</sup> Note that IC<sub>50</sub> data on MG63 have been previously reported in Rossi et al.; Molecules 2022, 27 [18].

In Table 1, the chemical structures of Lic-A and the selected chalcones are reported. The comparison of IC<sub>50</sub> values 48 h after treatment on both MG63 [18] and 143B cells is shown as well. The dose response curves on 143B cells are reported in figure 1SI. Interestingly, all compounds are effective, as their IC<sub>50</sub> values range from 5 to 20 µM, except for 1e whose IC<sub>50</sub> is 42.5 µM on MG63. Considering that chalcones are natural-like molecules, their activity at micromolar level is noteworthy. Moreover, while the activity of licochalcones against solid tumors is well documented [31], their effect on bone tumors and its potential mechanism/s of action have not been extensively studied [18–20].

Only three papers attest to the Lic-A cytotoxic activity against human osteosarcoma cells, including our previous work cited above. Therefore, chalcones antiproliferative activity on 143B osteosarcoma cell line, characterized by high metastatic potential, makes them promising anticancer candidates and deserving of further study.

### 3.2. Characterization of multicellular tumor spheroids

Preclinical data from 2D culture models are encouraging but often unreliable *in vivo* due to the lack of complex cytoarchitecture and tumor microenvironment considerations. Indeed, less than 10 % of new anticancer drug candidates that enter phase I trials are subsequently approved by the Food and Drug Administration [32]. One of the main challenges facing the development of a new anticancer treatment is the transition from preclinical discovery to clinical practice, the so-called 'from bench to bedside'. It is therefore crucial to develop advanced models based on 3D cultures, capable of recreating not only the spatial structure, but also the oxygen, nutrient and waste gradients found *in vivo* [33].

To have suitable MG63 and 143B OS 3D models, different cell seeding densities (4000, 2000, and 500 cells/well) were investigated. Within 24 h of seeding, compact spheroids formed consistently across all seeding densities for both cell lines (Fig. 1A). Interestingly, MCTS increased their size depending on cell type: 143B-MCTS grew very rapidly with respect to MG63-MCTS (Fig. 1B). To obtain a comparable

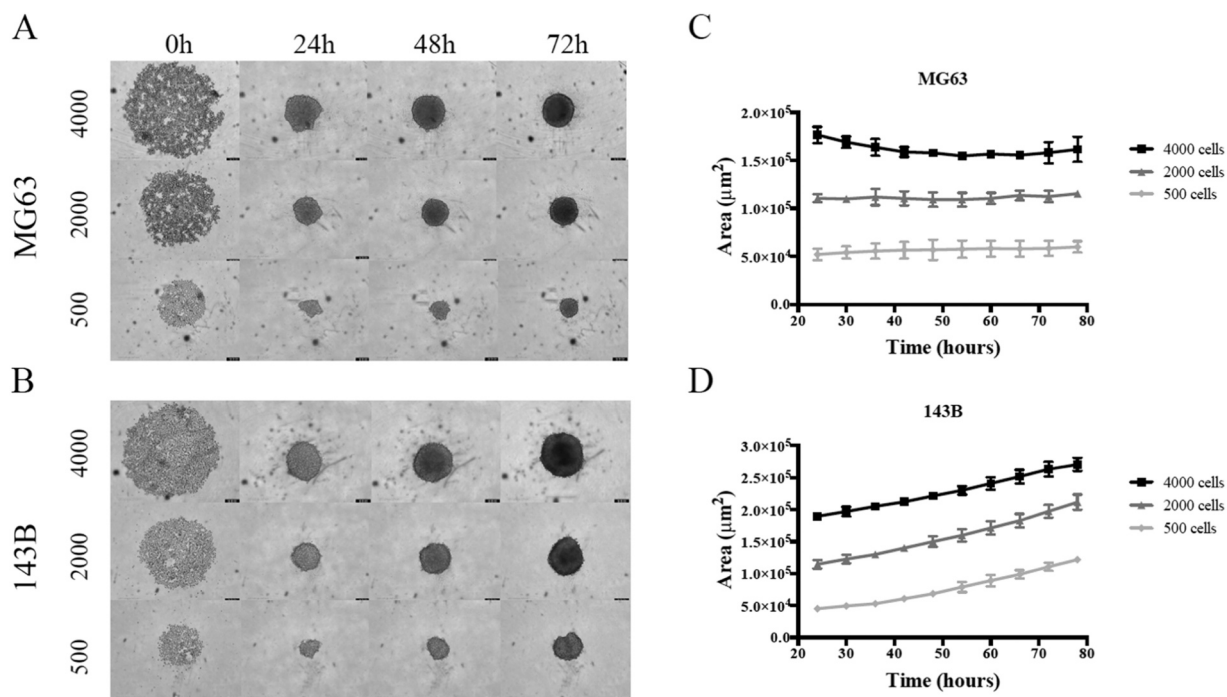


**Fig. 1. MCTS morphology and characterization.** Phase contrast images of spheroids generated at different cell densities (4000, 2000 and 500 cells) from MG63 (A) and 143B (B) at 0, 24, 48, and 72 h. Spheroid area from 24 to 78 h calculated through IncucyteZoom Software, for MG63 cells (C) and 143B cells (D). Values are expressed as mean  $\pm$  SD (n=6).

spheroid size for the treatment, different cell seeding densities were selected: 4000 cells/well for MG63 and 2000 cells/well for 143B. At 72 h an area of  $15.8 \pm 1.1 \times 10^4$  and of  $19.7 \pm 1.0 \times 10^4 \mu\text{m}^2$  was measured for MG63 and 143B, respectively.

MCTS morphological analysis, explored by confocal microscopy, highlighted the compactness of the spheroids and the homogeneous cell distribution throughout their entire volume (Fig. 2). It is worth noting that 143B-MCTS were denser, if compared to MG63-MCTS, probably due to their greater proliferation and smaller cell size. The results confirm the suitability of these 3D models for testing new anticancer agents, reflecting the peculiar characteristics of the cell types.

### 3.3. Antiproliferative effect of chalcones on 3D cell culture models

To find out the chalcone effective concentration, MCTS were treated with a concentration range from 5 to 160  $\mu\text{M}$ . As shown in Fig. 3A, a significant decrease in metabolic activity was observed in MG63-MCTS after treatment with Lic-A, 1i and 1k at 160  $\mu\text{M}$  ( $p < 0.001$ ). Furthermore, Lic-A, 1i, 1k, 1o and 1q showed a consistent effect ( $p < 0.001$ ), already detected at 80  $\mu\text{M}$  in 143B-MCTS (Fig. 3B). To evaluate the chalcones' effects on the 3D models, the resazurin assay was chosen instead of MTT test, previously used on the 2D cell culture. Several studies show that the resazurin and MTT methods exhibit comparable

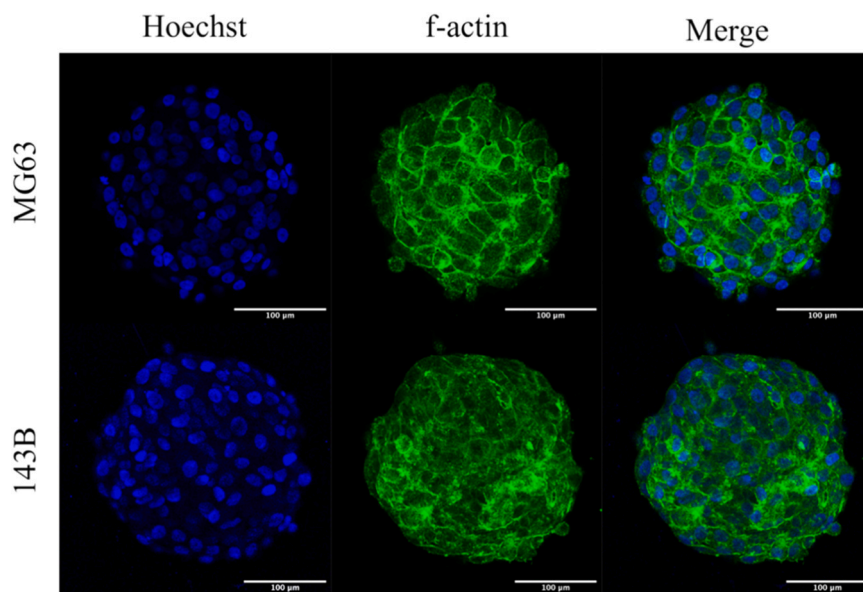
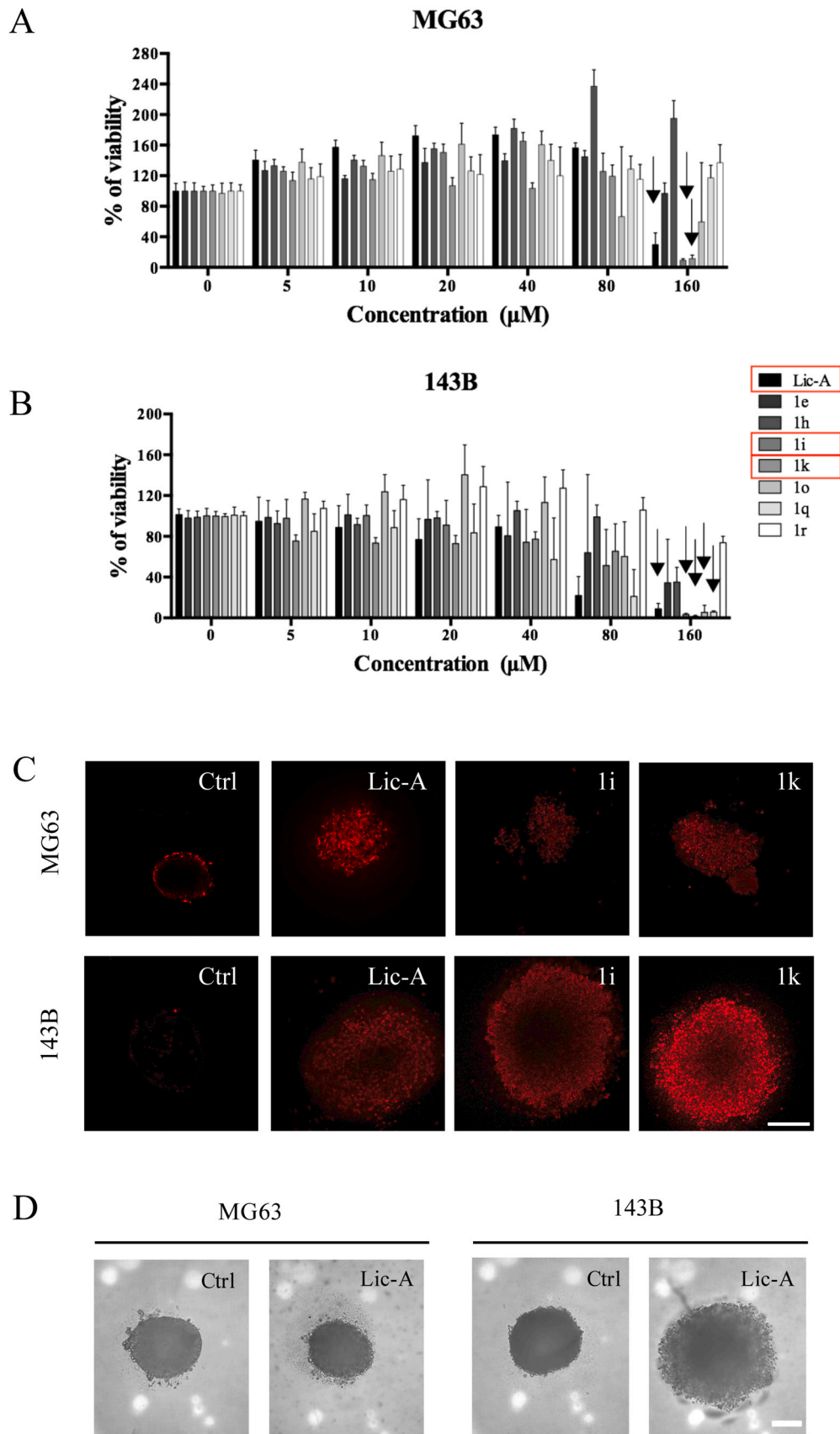


**Fig. 2. MCTS confocal microscopy analysis.** Representative images of the spheroidal models: nuclei are stained with Hoechst (blue) and F-actin filaments are stained with phalloidin (green). Scale bar 100  $\mu\text{m}$ .



(caption on next page)

**Fig. 3. Comparative analysis of the cytotoxic effects of chalcones on MG63 and 143B MCTS.** Resazurin assay was performed 72 h after treatment with seven different concentrations (160, 80, 40, 20, 10, 5 and 0  $\mu\text{M}$ ) on MG63 (A) and 143B-MCTS (B). Black arrows indicate the concentrations at which the compounds exhibit cytotoxicity while the red boxes (in the legend) highlight the chalcones selected for apoptosis, autophagy, and invasiveness studies. Values are expressed as mean  $\pm$  SD (n=8). A two-way Anova against control was conducted (p values are reported in the discussion). Fluorescence confocal microscopy images of MCTS treated with 120  $\mu\text{M}$  of chalcones and stained with PI 72 h after treatment. (C). Representative phase images of MG63 (left) and 143B (right) MCTS after 72 h treatment with Lic-A (D). Scale bar 200  $\mu\text{m}$ .

linear patterns [34,35] However, compared to MTT, the resazurin assay is a non-destructive assay and allows cell metabolism to be monitored at different times, representing the test most frequently used on spheroids [36].

Currently, OS treatment is based on antitumor drugs not specific for this type of cancer. In clinical practice, patients are treated with first-line anticancer drugs, such as doxorubicin and cisplatin [37]. Therefore, it is of utmost importance to discover new anticancer molecules able to specifically act against OS cells in all their heterogeneity. Thus, for the following experiments Lic-A, 1i and 1k chalcones were selected, since they were effective on both MCTS models (red boxes in Fig. 3A-B). To confirm their cytotoxic effects, a viability assay was carried out. After 72 h of treatment with Lic-A, 1i and 1k, MCTS were stained with propidium iodide, a fluorescence probe which only penetrates dead cells. An intense red staining is appreciable for all the treated samples if compared to the control (Fig. 3C). Interestingly, the three compounds active in both osteosarcoma cell lines also showed good selectivity for tumor cells. Indeed, treatment of healthy human fibroblast spheroids did not produce cytotoxic effects. Notably, Lic-A induced a slight reduction in viability, but only at the highest concentration (160  $\mu\text{M}$ ). This result confirmed the suitability of the chalcones under study as promising anti-osteosarcoma agents (Fig. 2 SI).

From a morphological point of view, in response to effective anticancer treatment, the spheroid pattern may meet two fates: reduction in size [38], as observed in tumor spheroids treated with cisplatin, doxorubicin, 5-fluorouracil [39]; or loss of cell-cell contact, compactness and integrity, as reported for ovarian or breast spheroids treated with cisplatin and doxorubicin [40]. In accordance with this experimental evidence, it was observed that the MG63-MCTS along the death process remained intact and also appeared to shrink in size. On the other hand, 143B-MCTS after treatment with chalcones flaked off, the dead cells lost contact with each other and formed a ring around the smaller residual core (Fig. 3D). These results highlight the effectiveness of chalcones in inducing death in both cell types, albeit characterized by different morphological changes in response to treatment.

### 3.4. Effect of chalcones on apoptosis

Apoptosis is a programmed cell death process essential for

maintaining tissue homeostasis, development, and eliminating damaged or potentially harmful cells. An anticancer agent inducing apoptosis is highly desirable. Several studies have demonstrated that chalcones, and in particular Lic-A, exert their anti-tumor activity by inducing apoptosis [41–44].

To verify if the antiproliferative effect observed here culminates with apoptosis induction, the activity of executive caspases 3/7 was analyzed after treatment in both 2D and 3D cell models. An increase of caspase activity has been observed for all molecules in both MCTS models (Fig. 4). However, this was significant for Lic-A and 1k on MG63 cells (Fig. 4A) and for Lic-A alone on 143B cells (Fig. 4B). Interestingly, the same treatment seemed to have a higher apoptosis induction in 2D culture (Figure 3SI). These data are in line with the general evidence that results obtained in 2D cell cultures are attenuated in 3D models, supporting the need to screen new anticancer agents in 3D cultures, testing *in vivo* the most promising compounds [45].

### 3.5. Effect of chalcones on autophagy

Autophagy is an intracellular degradation process that eliminates and recycles damaged proteins and organelles. Although autophagy is a pro-survival mechanism, overactivated autophagy can lead to cell death [46]. Autophagy is recognized as a critical process in bone homeostasis [47], usually dysregulated in OS disease, that could act both as a pro- or antitumor mechanism. LC3 and p62 proteins were evaluated as markers of autophagy flux by western blot. LC3, in particular its phosphatidylethanolamine-conjugated form (LC3-II), plays a role in assembling phagophores and in the formation of autophagosomes. Conversely, p62 functions as a molecular bridge, connecting LC3 to ubiquitinated substrates, and facilitating their targeting for autophagic degradation.

To assess the ability of Lic-A, 1i, and 1k to modulate autophagy, MCTS were analyzed 24 h after treatment. Lic-A and 1k significantly increased LC3-II ( $p < 0.01$ ) and p62 ( $p < 0.05$ ), while no significant changes can be observed after treatment with 1i on 143B-MCTS, the most invasive cell line (Fig. 5). No significant autophagic effect was observed on MG63-MCTS (data not shown). Our data also show a significant increase of autophagy markers after treatment with Lic-A and 1k (both LC3-II and p62 for Lic-A, only p62 for 1k,  $p < 0.05$ ) even in co-

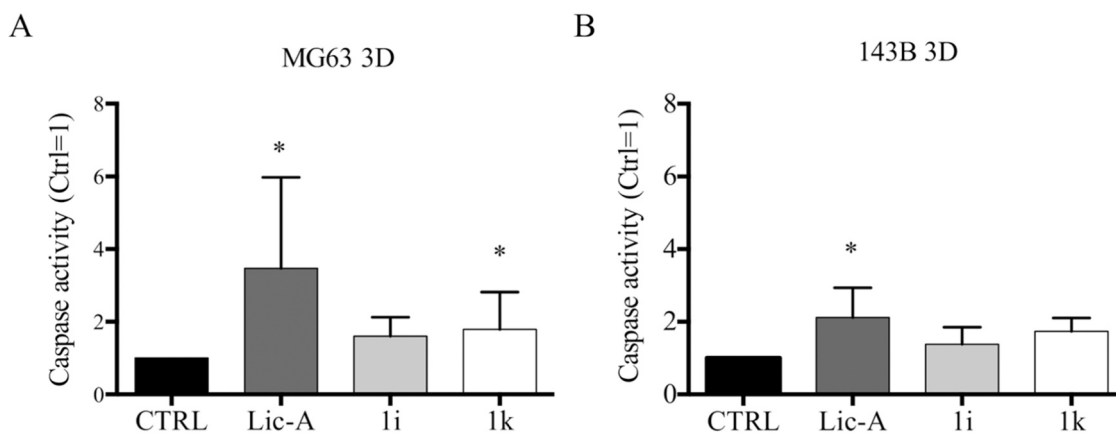


**Fig. 4. Apoptotic effect of chalcones on OS cell grown in 3D culture.** Caspase 3/7 activity was fluorometrically determined after treatment with Lic-A, 1i and 1k for 24 h. The analysis was performed on MG63 (A) and 143B (B) spheroids. Values are expressed as mean  $\pm$  SD (n=3). Friedman test against control was conducted. Significance was graphically reported as follows: \* $p < 0.05$ .

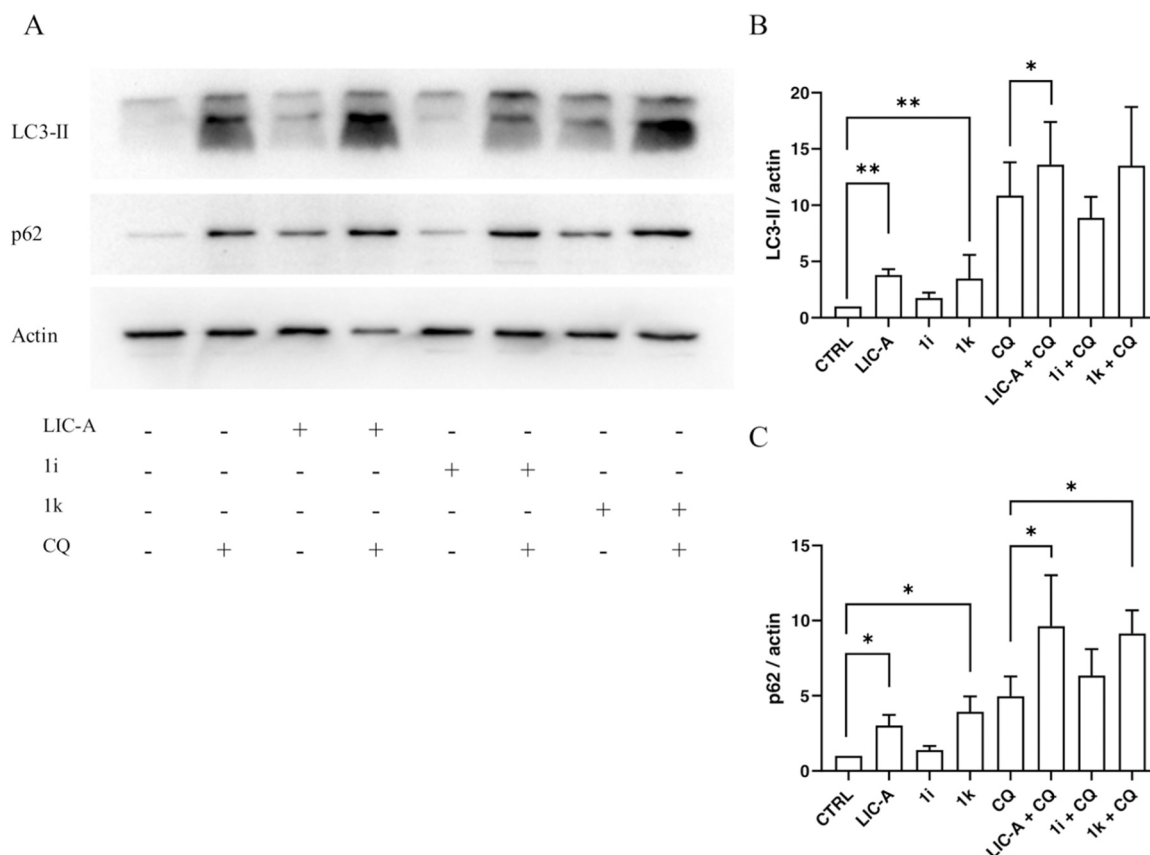


**Fig. 5. Autophagic effect of chalcones on 143B-MCTS.** Representative image of LC3-II, p62 and actin, as loading control, by western blot analysis after 24 h treatment (A). Cumulative data obtained with multiple experiments are reported in graphs showing relative quantification for LC3-II /actin (B) and p62/ actin (C). Values are expressed as mean  $\pm$  SD (n=4). A paired t-test was conducted against control, and CQ respectively. Significance was graphically reported as follows: \* p < 0.05 and \*\* p < 0.01.

treatment with CQ, thus confirming that these compounds stimulated autophagic turnover. Since autophagy is a highly dynamic pathway and therefore steady-state measurements can be difficult, current guidelines suggest comparing these findings under identical conditions in the presence of an autophagic flux inhibitor, such as CQ [28]. This strategy allows for the accumulation of the autophagic protein LC3-II and p62, thus ensuring a better observation by western blot analysis. Autophagy induction by chalcones has been reported in various solid tumors. Specifically, Shen *et al.* have reported the Lic-A autophagic effect in HOS osteosarcoma cell line [20], while Hang *et al.* have observed autophagy after treatment with Licochalcone B on U2OS cells [48].

Other authors have reported that Lic-A is able to inhibit the PI3K/Akt/mTOR signaling pathway, which in turn increases the expression of LC3-II protein and ultimately induces autophagy in MCF-7 cells [49].

Here we report the ability of Lic-A and 1k to promote autophagy in highly metastatic osteosarcoma cells. To the best of our knowledge, this is the first study demonstrating chalcone activity on 3D models of human osteosarcoma, in a condition that better mimics the tumor environment and therefore more likely to be reliable.

### 3.6. The effect of chalcones on OS cell invasiveness

Cell invasion consisting in the breaching of tissue barriers like endothelial basement membrane is a basic function of immune cells to respond and to prevent infections. Unfortunately, invasion is also used by cancer cells during disease progression triggering cell spreading and generating metastasis [50]. Cancer cell ability to metastasize and invade are peculiar features of aggressive tumors, such as OS, that often lead to a negative outcome for patients. As reported in the literature [29], 143B

cells exhibit a greater metastatic capacity than MG63 cells. Indeed, invasiveness is clearly appreciable for 143B cells, as shown in the quantitative analysis reported in Fig. 6. Data obtained for MG63 are reported in SI (Figure 4SI).

To assess the chalcone ability to reduce cell dissemination, an invasion assay on natural extracellular matrix-based hydrogel (Matrigel®) was performed. Three days after seeding, MCTS were embedded into Matrigel® and spheroid outgrowth was monitored over time. 143B showed high basal cell spreading proven by the massive migration of the cells from the spheroid body to the matrix. In contrast, the spreading ability of MCTS treated with Lic-A seems completely inhibited (Fig. 6A). In fact, neither the whole spheroid area, nor the invading cell area increased over time (Fig. 6B and C). Similarly, chalcone 1k inhibited cell spreading, although to a lesser extent. Finally, chalcone 1i showed no effect on invasion capacity, and no significant differences were appreciable in terms of whole spheroid and invading cell area compared to the control. These results demonstrate that Lic-A, in addition to decreasing proliferation, is also able to reduce the metastatic potential of human OS cells. This activity has already been reported for other solid tumors, such as breast [24,51] or lung cancer [52].

It is interesting to note that, in the control samples, thin filaments seem to invade the matrix. These are no more visible after treatment. It can be speculated that these structures are cytoplasmic protrusions known as invadopodia, structures having a key role in tumor metastatization. Indeed, invadopodia promote the proteolytic matrix degradation to favor cancer cell invasion, create space in the extracellular matrix to allow tumors growth by activating various growth factors [53].

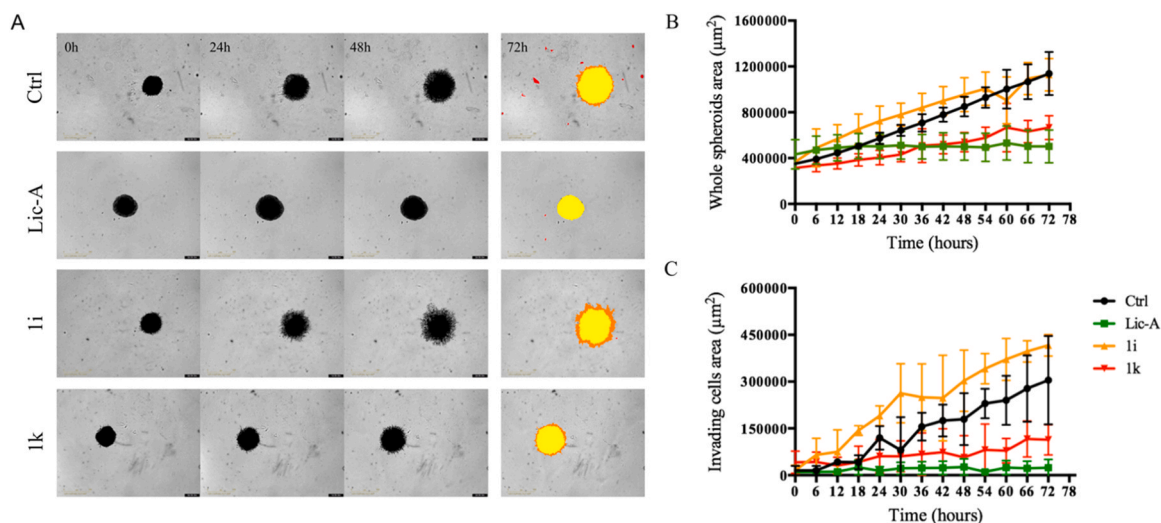


**Fig. 6. Invasion assay performed by Incucyte instrument.** Representative phase contrast images of 143B-MCTS embedded on Matrigel at 0, 24, 48 and 72 h of treatment. Images showing the analysis mask are reported on the right. The whole spheroid area is reported in yellow and the invading cell area in red (A). Whole spheroids area along time calculated through Incucyte® Zoom Software (B). Invading cell area calculated through Incucyte® Zoom Software (C). Values are expressed as mean  $\pm$  SD (n=3). A two-way Anova against control was conducted at the end point.  $p < 0.001$  for Lic-A and 1k.

#### 4. Conclusions

It has been accepted that the application of advanced 3D models will make the screening of anticancer compounds faster and more reliable, in line with the principles of refinement, reduction, and replacement (3 R) in research.

In this study an easily reproducible 3D model for the selection of potential anticancer agents against OS was obtained, proposing the switch from the 2D cell culture currently employed to 3D spheroid models.

Starting from a series of newly synthesized chalcones, the two most potent derivatives (1i and 1k), together with the parent compound Lic-A, were investigated for their ability to inhibit the proliferation of OS cells organized in MCTS. Our findings address the need to streamline the translation of a reduced number of molecules into preclinical studies, based on their antitumor activity in systems that closely mimic *in vivo* conditions. Additionally, the effectiveness of chalcone as a natural scaffold for generating potential antiproliferative agents has been demonstrated. In particular, chalcones exert their antiproliferative activity by inducing apoptosis and autophagy. Interestingly, they are capable of reducing cell invasion, which significantly contributes to the adverse prognosis of OS. To the best of our knowledge, Lic-A was tested on a 3D model for the first time, confirming its anticancer properties against human OS.

Further studies are underway to elucidate the signaling pathways and molecular targets responsible for the antitumor activity of chalcones in OS. In parallel, the MCTS model will be improved by incorporating other cell types and matrix components of the tumor microenvironment for a more reliable tumoroid 3D model.

#### Funding

This research was funded by the Italian Ministry of Health (Ministero della Salute), in the frame of the project 'Sviluppo di approcci innovativi ed alternativi alla modellistica animale in ambito tossicologico, oncologico e per disturbi del neurosviluppo'. In particular, the research activities were carried out in WP5 'Modelli complessi tridimensionali di osteosarcoma umano per sostituire la sperimentazione animale negli studi preclinici' (P.I. Prof. Emil Malucelli). The work of M.R. was funded by the Department of Pharmacy and Biotechnology, University of Bologna with the grant entitled 'Development of osteosarcoma 3D cell

cultures for the screening of new chemotherapeutics' (BIR19).

#### CRediT authorship contribution statement

**Martina Rossi:** Conceptualization, Data curation, Methodology, Validation, Visualization, Writing - original draft. **Cristina Pellegrino:** Investigation. **Martyna Malgorzata Ryzdzyk:** Investigation. **Giovanna Farruggia:** Validation, Visualization. **Dario De Biase:** Data curation, Investigation. **Silvia Cetrullo:** Data curation, Validation, Visualization. **Stefania D'Adamo:** Data curation, Investigation. **Alessandra Bisi:** Writing - review & editing. **Paolo Blasi:** Supervision, Funding acquisition, Writing - review & editing, Project administration. **Emil Malucelli:** Supervision, Funding acquisition, Writing - review & editing, Project administration. **Concettina Cappadone:** Conceptualization, Methodology, Validation, Supervision, Writing - review & editing. **Silvia Gobbi:** Supervision, Funding acquisition, Project administration.

#### Declaration of Competing Interest

The authors declare that they have no known competing financial interests or personal relationships that could have appeared to influence the work reported in this paper.

#### Data Availability

Data will be made available on request.

#### Acknowledgements

The authors wish to express their thanks to the Centre for Applied Biomedical Research, University of Bologna for its support, specifically to Dott. Biljana Petrovic for assistance with the Incucyte® analysis. Authors would also like to thank Dott. Manuela Voltattorni for the confocal microscopy analysis.

#### Appendix A. Supporting information

Supplementary data associated with this article can be found in the online version at [doi:10.1016/j.biopha.2024.117284](https://doi.org/10.1016/j.biopha.2024.117284).



## References

- [1] M. Kansara, M.W. Teng, M.J. Smyth, D.M. Thomas, Translational biology of osteosarcoma, *Nat. Rev. Cancer* 14 (2014) 722–735, <https://doi.org/10.1038/nrc3838>.
- [2] R.A. Durfee, M. Mohammed, H.H. Luu, Review of osteosarcoma and current management, *Rheuma Ther.* 3 (2016) 221–243, <https://doi.org/10.1007/s40744-016-0046-y>.
- [3] L. Mirabello, R.J. Troisi, S.A. Savage, Osteosarcoma incidence and survival rates from 1973 to 2004: data from the Surveillance, Epidemiology, and End Results Program, *Cancer* 115 (2009) 1531–1543, <https://doi.org/10.1002/cncr.24121>.
- [4] J. Rodrigues, B. Sarmiento, C.L. Pereira, Osteosarcoma tumor microenvironment: the key for the successful development of biologically relevant 3D in vitro models, *Vitr. Models* (2022) doi.org/10.1007/s44164-022-00008-x, 5–27, doi:10.1007/s44164-022-00008-x.
- [5] K.H. Lee, T.H. Kim, Recent advances in multicellular tumor spheroid generation for drug screening, *Biosens. (Basel)* 11 (2021), <https://doi.org/10.3390/bios11110445>.
- [6] M. Rossi, P. Blasi, Multicellular tumor spheroids in nanomedicine research: a perspective, *Front Med Technol.* 4 (2022) 909943, <https://doi.org/10.3389/fmedt.2022.909943>.
- [7] V. Sandhu, D. Bakkalci, S. Wei, U. Cheema, Enhanced biomimetics of three-dimensional osteosarcoma models: a scoping review, *Cancers (Basel)* 16 (2023), <https://doi.org/10.3390/cancers16010164>.
- [8] A. De Luca, L. Raimondi, F. Salamanna, V. Carina, V. Costa, D. Bellavia, R. Alessandro, M. Fini, G. Giavaresi, Relevance of 3d culture systems to study osteosarcoma environment, *J. Exp. Clin. Cancer Res* 37 (2018) 2, <https://doi.org/10.1186/s13046-017-0663-5>.
- [9] R. Michalkova, L. Mirossay, M. Gazdova, M. Kello, J. Mojzic, Molecular mechanisms of antiproliferative effects of natural chalcones, *Cancers (Basel)* 13 (2021), <https://doi.org/10.3390/cancers13112730>.
- [10] S. Shukla, A.K. Sood, K. Goyal, A. Singh, V. Sharma, N. Guliya, S. Gulati, S. Kumar, Chalcone scaffolds as anticancer drugs: a review on molecular insight in action of mechanisms and anticancer properties, *Anticancer Agents Med Chem.* 21 (2021) 1650–1670, <https://doi.org/10.2174/1871520620999201124212840>.
- [11] M. Tobeiha, A. Rajabi, A. Raisi, M. Mohajeri, S.M. Yazdi, A. Davoodvandi, F. Aslanbeigi, M. Vaziri, M.R. Hamblin, H. Mirzaei, Potential of natural products in osteosarcoma treatment: focus on molecular mechanisms, *Biomed. Pharm.* 144 (2021) 112257, <https://doi.org/10.1016/j.biopha.2021.112257>.
- [12] P. Singh, A. Anand, V. Kumar, Recent developments in biological activities of chalcones: a mini review, *Eur. J. Med Chem.* 85 (2014) 758–777, <https://doi.org/10.1016/j.ejmech.2014.08.033>.
- [13] C. Zhuang, W. Zhang, C. Sheng, W. Zhang, C. Xing, Z. Miao, Chalcone: a privileged structure in medicinal chemistry, *Chem. Rev.* 117 (2017) 7762–7810, <https://doi.org/10.1021/acs.chemrev.7b00020>.
- [14] Y. Ouyang, J. Li, X. Chen, X. Fu, S. Sun, Q. Wu, Chalcone derivatives: role in anticancer therapy, *Biomolecules* 11 (2021), <https://doi.org/10.3390/biom11060894>.
- [15] T. Constantinescu, C.N. Lungu, Anticancer activity of natural and synthetic chalcones, *Int J. Mol. Sci.* 22 (2021), <https://doi.org/10.3390/ijms222111306>.
- [16] B. Zhou, Xing, C. Diverse molecular targets for chalcones with varied bioactivities, *Med Chem. (Los Angel)* 5 (2015) 388–404, <https://doi.org/10.4172/2161-0444.1000291>.
- [17] M.N. Gomes, E.N. Muratov, M. Pereira, J.C. Peixoto, L.P. Rosseto, P.V.L. Cravo, C. H. Andrade, B.J. Neves, Chalcone derivatives: promising starting points for drug design, *Molecules* 22 (2017), <https://doi.org/10.3390/molecules22081210>.
- [18] M. Rossi, C. Cappadone, G. Picone, A. Bisi, G. Farruggia, F. Belluti, P. Blasi, S. Gobbi, E. Malucelli, Natural-like chalcones with antitumor activity on human MG63 osteosarcoma cells, *Molecules* 27 (2022), <https://doi.org/10.3390/molecules27123751>.
- [19] R.C. Lin, S.F. Yang, H.L. Chiou, S.C. Hsieh, S.H. Wen, K.H. Lu, Y.H. Hsieh, Licochalcone A-induced apoptosis through the activation of p38MAPK pathway mediated mitochondrial pathways of apoptosis in human osteosarcoma cells in vitro and in vivo, *Cells* 8 (2019), <https://doi.org/10.3390/cells8111441>.
- [20] T.S. Shen, Y.K. Hsu, Y.F. Huang, H.Y. Chen, C.P. Hsieh, C.L. Chen, Licochalcone A suppresses the proliferation of osteosarcoma cells through autophagy and ATM-Chk2 activation, *Molecules* 24 (2019), <https://doi.org/10.3390/molecules24132435>.
- [21] X. Liu, Y. Xing, M. Li, Z. Zhang, J. Wang, M. Ri, C. Jin, G. Xu, L. Piao, H. Jin, et al., Licochalcone A inhibits proliferation and promotes apoptosis of colon cancer cell by targeting programmed cell death-ligand 1 via the NF-kappaB and Ras/Raf/MEK pathways, *J. Ethnopharmacol.* 273 (2021) 113989 <https://doi.org/10.1016/j.jep.2021.113989>.
- [22] H. Shen, G. Zeng, G. Tang, X. Cai, L. Bi, C. Huang, Y. Yang, Antimetastatic effects of licochalcone A on oral cancer via regulating metastasis-associated proteases, *Tumour Biol.* 35 (2014) 7467–7474, <https://doi.org/10.1007/s13277-014-1985-y>.
- [23] C. Qiu, T. Zhang, W. Zhang, L. Zhou, B. Yu, W. Wang, Z. Yang, Z. Liu, P. Zou, G. Liang, Licochalcone A inhibits the proliferation of human lung cancer cell lines A549 and H460 by inducing G2/M cell cycle arrest and ER stress, *Int J. Mol. Sci.* 18 (2017), <https://doi.org/10.3390/ijms18081761>.
- [24] L.F. Bortolotto, F.R. Barbosa, G. Silva, T.A. Bitencourt, R.O. Beleboni, S.J. Baek, M. Marins, A.L. Fachin, Cytotoxicity of trans-chalcone and licochalcone A against breast cancer cells is due to apoptosis induction and cell cycle arrest, *Biomed. Pharm.* 85 (2017) 425–433, <https://doi.org/10.1016/j.biopha.2016.11.047>.
- [25] Y.J. Fan, W.X. Zong, The cellular decision between apoptosis and autophagy, *Chin. J. Cancer* 32 (2013) 121–129, <https://doi.org/10.5732/cjc.012.10106>.
- [26] S. Cetrullo, S. D'Adamo, V. Panichi, R.M. Borzi, C. Pignatti, F. Flamigni, Modulation of Fatty Acid-related Genes in the Response of H9c2 cardiac cells to palmitate and n-3 polyunsaturated fatty acids, *Cells* 9 (2020), <https://doi.org/10.3390/cells9030537>.
- [27] S. Cetrullo, S. D'Adamo, S. Guidotti, R.M. Borzi, F. Flamigni, Hydroxytyrosol prevents chondrocyte death under oxidative stress by inducing autophagy through sirtuin 1-dependent and -independent mechanisms, *Biochim Biophys. Acta* 1860 (2016) 1181–1191, <https://doi.org/10.1016/j.bbagen.2016.03.002>.
- [28] D.J. Klionsky, A.K. Abdel-Aziz, S. Abdelfatah, M. Abdellatif, A. Abdoli, S. Abel, H. Abeliovich, M.H. Abildgaard, Y.P. Abudu, A. Acevedo-Aroza, et al., Guidelines for the use and interpretation of assays for monitoring autophagy (4th edition), *Autophagy* 17 (1) (2021) 1–382, <https://doi.org/10.1080/15548627.2020.1797280>.
- [29] A.B. Mohseny, I. Machado, Y. Cai, K.L. Schaefer, M. Serra, P.C. Hogendoorn, A. Llombart-Bosch, A.M. Cleton-Jansen, Functional characterization of osteosarcoma cell lines provides representative models to study the human disease, *Lab Invest* 91 (2011) 1195–1205, <https://doi.org/10.1038/labinvest.2011.72>.
- [30] D. Malvi, F. Vasuri, T. Maloberti, V. Sanza, A. De Leo, A. Fornelli, M. Masetti, C. Benini, R. Lombardi, M.F. Offi, et al., Molecular characterization of pancreatic ductal adenocarcinoma using a next-generation sequencing custom-designed multigene panel, *Diagn. (Basel)* 12 (2022), <https://doi.org/10.3390/diagnostics12051058>.
- [31] N. Deng, M. Qiao, Y. Li, F. Liang, J. Li, Y. Liu, Anticancer effects of licochalcones: a review of the mechanisms, *Front Pharm.* 14 (2023) 1074506, <https://doi.org/10.3389/fphar.2023.1074506>.
- [32] M. Zanon, M. Cortesi, A. Zamagni, C. Arienti, S. Pignatta, A. Tesi, Modeling neoplastic disease with spheroids and organoids, *J. Hematol. Oncol.* 13 (2020) 97, <https://doi.org/10.1186/s13045-020-00931-0>.
- [33] B.W. Huang, J.Q. Gao, Application of 3D cultured multicellular spheroid tumor models in tumor-targeted drug delivery system research, *J. Control Release* 270 (2018) 246–259, <https://doi.org/10.1016/j.jconrel.2017.12.005>.
- [34] X. Gong, Z. Liang, Y. Yang, H. Liu, J. Ji, Y. Fan, A resazurin-based, nondestructive assay for monitoring cell proliferation during a scaffold-based 3D culture process, *Regen. Biomater.* 7 (3) (2020) 271–281, <https://doi.org/10.1093/rb/rbaa002>.
- [35] K. Präbst, H. Engelhardt, S. Ringgler, H. Hübner, Basic colorimetric proliferation assays: MITT, WST, and resazurin, *Methods Mol. Biol.* 1601 (2017) 1–17, [https://doi.org/10.1007/978-1-4939-6960-9\\_1](https://doi.org/10.1007/978-1-4939-6960-9_1).
- [36] S.N. Rampersad, Multiple applications of Alamar Blue as an indicator of metabolic function and cellular health in cell viability bioassays, *Sens. (Basel)* 12 (9) (2012) 12347–12360, <https://doi.org/10.3390/s120912347>.
- [37] Z. Hu, S. Wen, Z. Huo, Q. Wang, J. Zhao, Z. Wang, Y. Chen, L. Zhang, F. Zhou, Z. Guo, et al., Current status and prospects of targeted therapy for osteosarcoma, *Cells* 11 (2022), <https://doi.org/10.3390/cells11213507>.
- [38] B. Patra, C.C. Peng, W.H. Liao, C.H. Lee, Y.C. Tung, Drug testing and flow cytometry analysis on a large number of uniform sized tumor spheroids using a microfluidic device, *Sci. Rep.* 6 (2016) 21061, <https://doi.org/10.1038/srep21061>.
- [39] A. Senrnung, S. Lalwani, D. Janjua, T. Tripathi, J. Kaur, N. Ghuratia, N. Aggarwal, A. Chhokar, J. Yadav, A. Chaudhary, et al., 3D tumor spheroids: morphological alterations a yardstick to anti-cancer drug response, *Vitr. Models* (2023) doi.org/10.1007/s44164-023-00059-8, 219–248, doi:doi.org/10.1007/s44164-023-00059-8.
- [40] R. Akasov, D. Zaytseva-Zotova, S. Burov, M. Leko, M. Döntenwill, M. Chiper, T. Vandamme, E. Markvicheva, Formation of multicellular tumor spheroids induced by cyclic RGD-peptides and use for anticancer drug testing in vitro, *Int J. Pharm.* 506 (2016) 148–157, <https://doi.org/10.1016/j.ijpharm.2016.04.005>.
- [41] J. Wang, Y.S. Zhang, K. Thakur, S.S. Hussain, J.G. Zhang, G.R. Xiao, Z.J. Wei, Licochalcone A from licorice root, an inhibitor of human hepatoma cell growth via induction of cell apoptosis and cell cycle arrest, *Food Chem. Toxicol.* 120 (2018) 407–417, <https://doi.org/10.1016/j.fct.2018.07.044>.
- [42] G. Zeng, H. Shen, Y. Yang, X. Cai, W. Xun, Licochalcone A as a potent antitumor agent suppresses growth of human oral cancer SCC-25 cells in vitro via caspase-3 dependent pathways, *Tumour Biol.* 35 (7) (2014) 6549–6555, <https://doi.org/10.1007/s13277-014-1877-1>.
- [43] S.H. Hong, H.J. Cha, H. Hwang-Bo, M.Y. Kim, S.Y. Kim, S.Y. Ji, J. Cheong, C. Park, H. Lee, G.Y. Kim, S.K. Moon, et al., Anti-proliferative and pro-apoptotic effects of licochalcone A through ROS-mediated cell cycle arrest and apoptosis in human bladder cancer cells, *Int J. Mol. Sci.* 20 (15) (2019) 3820, <https://doi.org/10.3390/ijms20153820>.
- [44] J.J. Cho, J.I. Chae, G. Yoon, K.H. Kim, J.H. Cho, S.S. Cho, Y.S. Cho, J.H. Shim, Licochalcone A, a natural chalconoid isolated from *Glycyrrhiza inflata* root, induces apoptosis via Sp1 and Sp1 regulatory proteins in oral squamous cell carcinoma, *Int J. Oncol.* 45 (2) (2014) 667–674, <https://doi.org/10.3892/ijo.2014.2461>.
- [45] E.M. Tosca, D. Ronchi, D. Facciolo, P. Magni, Replacement, reduction, and refinement of animal experiments in anticancer drug development: the contribution of 3D in vitro cancer models in the drug efficacy assessment, *Biomedicines* 11 (4) (2023) 1058, <https://doi.org/10.3390/biomedicines11041058>.
- [46] O. Camuzard, S. Santucci-Darmanin, G.F. Carle, V. Pierrefite-Carle, Role of autophagy in osteosarcoma, *J. Bone Oncol.* 16 (2019) 100235, <https://doi.org/10.1016/j.jbo.2019.100235>.
- [47] V. Pierrefite-Carle, S. Santucci-Darmanin, V. Breuil, O. Camuzard, G.F. Carle, Autophagy in bone: self-eating to stay in balance, *Ageing Res Rev.* 24 (2015) 206–217, <https://doi.org/10.1016/j.arr.2015.08.004>.

- [48] Z. Huang, G. Jin, Licochalcone B induced apoptosis and autophagy in osteosarcoma tumor cells via the inactivation of PI3K/AKT/mTOR pathway, *Biol. Pharm. Bull.* 45 (6) (2022) 730–737, <https://doi.org/10.1248/bpb.b21-00991>.
- [49] L. Xue, W.J. Zhang, Q.X. Fan, L.X. Wang, Licochalcone A inhibits PI3K/Akt/mTOR signaling pathway activation and promotes autophagy in breast cancer cells, *Oncol. Lett.* 15 (2) (2018) 1869–1873, <https://doi.org/10.3892/ol.2017.7451>.
- [50] K. Karamanou, M. Franchi, D. Vynios, S. Brézillon, Epithelial-to-mesenchymal transition and invadopodia markers in breast cancer: Lumican a key regulator, *Semin Cancer Biol.* 62 (2020) 125–133, <https://doi.org/10.1016/j.semcancer.2019.08.003>.
- [51] W.C. Huang, H.H. Su, L.W. Fang, S.J. Wu, C.J. Liou, Licochalcone A inhibits cellular motility by suppressing e-cadherin and MAPK signaling in breast cancer, *Cells* 8 (3) (2019) 218, <https://doi.org/10.3390/cells8030218>.
- [52] H.C. Huang, L.L. Tsai, J.P. Tsai, S.C. Hsieh, S.F. Yang, J.T. Hsueh, Y.H. Hsieh, Licochalcone A inhibits the migration and invasion of human lung cancer cells via inactivation of the Akt signaling pathway with downregulation of MMP-1/-3 expression, *Tumour Biol.* 35 (12) (2014) 12139–12149, <https://doi.org/10.1007/s13277-014-2519-3>.
- [53] E.K. Paterson, S.A. Courtneidge, Invadosomes are coming: new insights into function and disease relevance, *FEBS J.* 285 (1) (2018) 8–27, <https://doi.org/10.1111/febs.14123>.